Common Development of Prisms, Anti-Prisms, Tetrahedra, and Wedges

Amartya Shankha Biswas[*]   Erik D. Demaine[*]

Abstract

We construct an uncountably infinite family of unfoldings, each of which can be folded into twelve distinct convex solids, while also tiling the plane.

1   Introduction

The problem of folding polygons into convex polyhedra was posed by Lubiw and O'Rourke [5]. Since then there have been several results about polygons that can fold into multiple distinct polyhedra. One of the first results in this field was by Mitani and Uehara [6], who construct a countably infinite family of unfoldings, each of which can fold into two different orthogonal boxes with integer sides. This was further expanded in [1] and [8] to produce countably infinite families that fold into three different boxes. Other results investigate unfoldings between Platonic solids [7] and between the regular tetrahedron and each Johnson-Zalgaller solid [3].

All of these common unfoldings, however, fold into only a small number of polyhedra. A notable exception is the two examples in [4, sec. 25.6–25.7]: the Latin Cross folds into 23 distinct convex polyhedra, while the square folds into six uncountable families of convex polyhedra. These case studies, however, do not easily generalize to families of unfoldings. It is also relatively easy to make a common unfolding of infinitely many tetrahedra, from any rectangle, but this relies on the simple mechanism of rolling belts and all resulting polyhedra are combinatorially equivalent. Another result that concerns a large number of polyhedra is the common development of 22 pentacubes [2]; however, most of these polycubes are non-convex. This still leaves open the problem of finding large families of common developments of a large number of convex polyhedra; see Sections 2.1–2.2 for further discussion.

We construct a common development that can fold into **twelve** different convex polyhedra, in five different combinatorial classes. Additionally, we show that there is an ***uncountably* infinite** family of such developments, each giving rise to twelve different convex polyhedra.

In particular, two of these polyhedra are orthogonal boxes (specifically square prisms). So, if we consider

only rational edge lengths, this results in a new infinite family of developments that are common unfoldings of two different (integer-sided) boxes. This is very similar to the results in [6], since we will only be cutting along grid lines.

Another useful property considered in [6, 1, 8, 3] is whether the development tiles the plane. This is a practically important consideration, because it makes the development simple and efficient to fabricate from a sheet of material (no wastage). Our development does in fact tile the plane (Figure 1).

2   Development

The construction of our development starts with a rectangle of paper with size $L \times W$. We assume without loss of generality that $L > W$ and $W = 1$. All instances of $W \neq 1$ can be obtained by scaling the construction appropriately.

We then add square tabs to each set of opposite sides, such that each side has four equally spaced tabs (Figure 1). The tabs on the side with length L are squares of length $L/8$, and the ones on the adjacent sides are of length $W/8 = 1/8$. The tabs on the longer (L) side are shifted by a certain length in order to leave space for the smaller set of tabs (Figure 1). The shift has to be at least $1/8$ to accommodate this, and the maximum possible shift is $L/8$. This means that we require $L > 1$ for the construction to be feasible. On the other hand, the larger tabs extend to a distance $L/8$ into the paper, which also requires that $L/8 < 1 \implies L < 8$. This allows us to bound the aspect ratio $L = L/W$ of the development:

$$1 < L < 8.$$

In our construction, we set the shift distance L_{shift} as

$$L_{shift} = \frac{L/8 + W/8}{2}.$$

The final construction is shown in Figure 1.

The complementary tabs ensure that the pattern can still tile the plane. As an important consequence, this also allow us to "stitch" two opposite sides together without any gaps. This will allow us to pick either pair of opposite sides, and glue them together to form two different cylinders.

We will refer to the cylinder formed by folding around the L side as the L-cylinder, and the one folded around
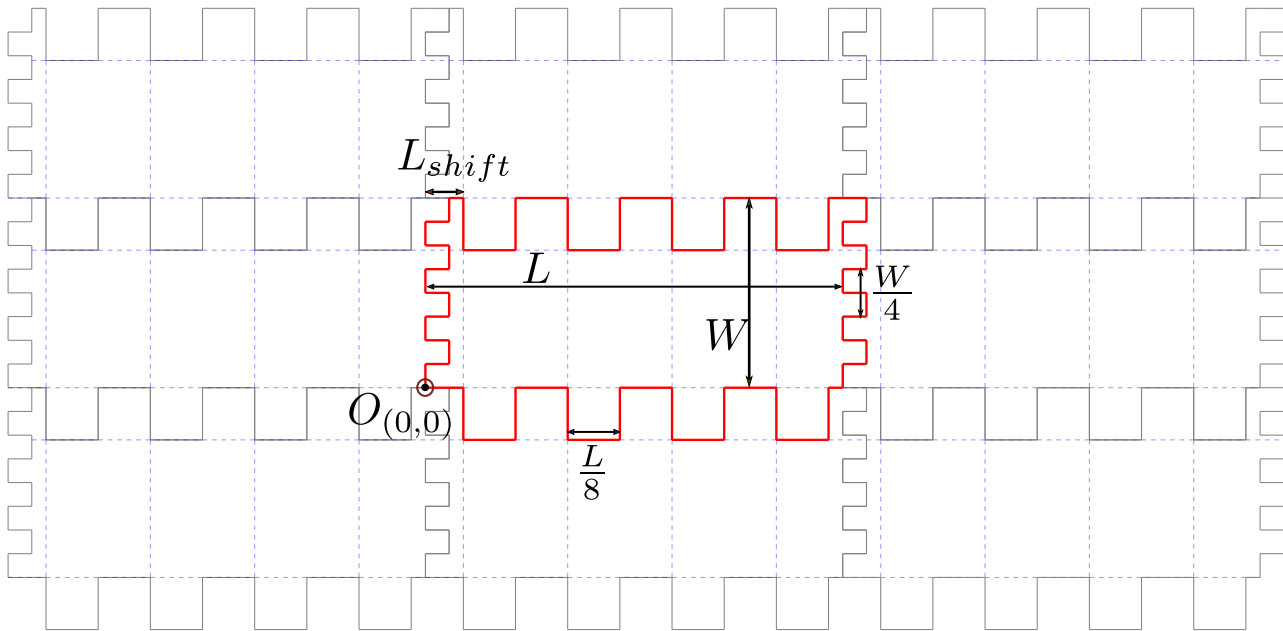
Figure 1: The development is constructed by adding tabs to an $L \times W$ rectangle—four tabs on each side, where opposite sides have complementary tabs. It tiles the plane. The blue dotted creases form one of the possible prisms.
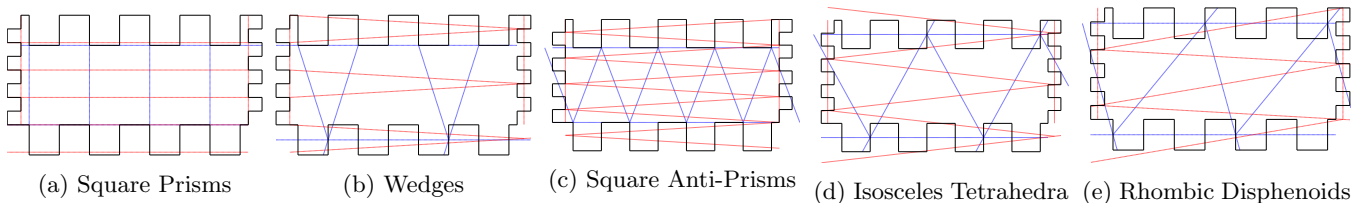

(a) Square Prisms   (b) Wedges   (c) Square Anti-Prisms   (d) Isosceles Tetrahedra   (e) Rhombic Disphenoids

Figure 2: Crease patterns for each of the possible foldings of Figure 1. The blue creases correspond to the solid formed by staring with the L-cylinder, and the red creases correspond to the solid formed by staring with the W-cylinder.

the W side as the W-cylinder. These cylinders have complementary sets of tabs on either end. We can close the ends in two different ways. The obvious closing is performed by folding down each of the square tabs by 90° to form a square end cap (Figure 3b). Note that there are actually two different ways to close the square. We can rotate the corners by 45°, and obtain a reflected version of the fold pattern (Figure 3c). The different possible orientations of the square are shown in Figure 5a.

Another way to close the end is to fold the tabs in half and form a straight line (Figure 3a). There are four possible orientations of the line zip, which are formed by varying the endpoints of the zip line (Figure 5b).

By closing the ends in different ways, we can obtain a large class of convex polyhedra. Each of these will be explained in detail in the following sections.

- **Square prism** — We can close both ends of the cylinder into squares that line up.

- **Square anti-prism** — Same as above, but one of

the squares is rotated by 45°.

- **Isosceles tetrahedra** — We close the ends of the cylinders by zipping them into orthogonal lines.

- **Rhombic disphenoids** — We zip the two ends into non-orthogonal lines. Since this solid is chiral, there are two possible foldings. This is essentially a tetrahedron with congruent scalene faces.

- **Obtuse wedges** — We close one of the ends into a square and the other one into a line.

Each of these constructions can be performed by starting with either cylinder. So, we obtain a total of $2 \times 5 = 10$ different convex polyhedra from this unfolding.
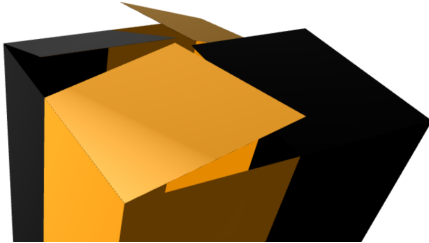
Further, the rhombic disphenoids have distinct mirror images which can also be constructed (by turning the folding inside out). This brings the total number of possible foldings to 12. Figure 2 gives the crease patterns for each of these shapes.

(a) Zippng the end of the cylinder into a line. See also Figure 9b.
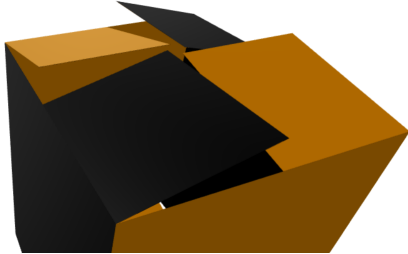
(b) Closing end into square

(c) Square rotated by $\pi/4$

Figure 3: The three different ways to close the end of a cylinder. Note that the line zipping can also be performed in four different locations (Figure 5b).

Theorem 1. *There is an uncountably infinite family of common developments for the aforementioned twelve polyhedra. Moreover, each member of this family can tile the plane.*

Proof. The development tiles the plane because we start with a rectangle (which tiles the plane), and add tabs, where each tab is added along with its complement. This preserves the tiling property. Since we can vary the length L continuously in the interval $(1, 8)$, this is an uncountable family. The subsequent sections elaborate on the construction of the twelve solids. □

2.1 Comparison to Rolling Belts

Rolling belts offer a trivial way to obtain uncountably infinite polyhedra from the same unfolding. Start with an arbitrary rectangle, and glue opposite sides to form a cylinder. Then the two ends of the cylinder can be zipped in (uncountable) infinitely many ways, to obtain an infinite family of tetrahedron foldings.

This construction is somewhat "uninteresting" because it relies on rolling belts. One way to formalize this is to consider the gluing tree [4] corresponding to each folding, which is the same for all of the tetrahedra
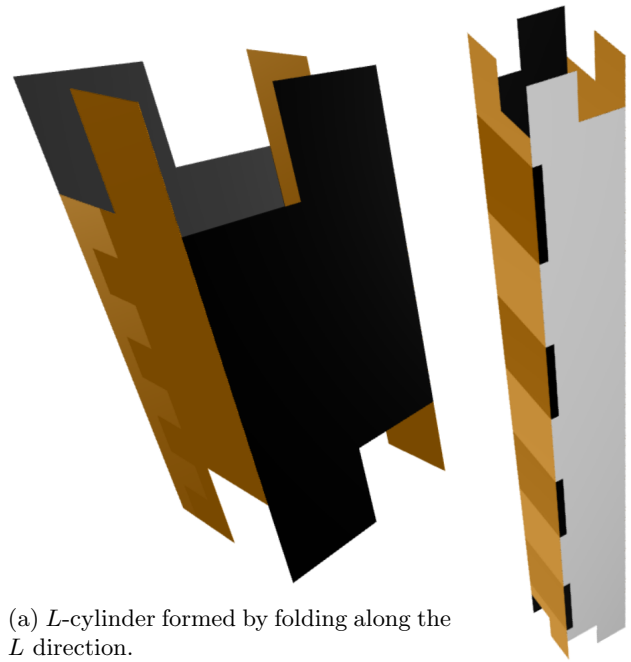
(a) L-cylinder formed by folding along the L direction.

(b) W-cylinder.

Figure 4: We start the construction by folding the development into a cylinder, and attaching the two ends using one set of complementary tabs.
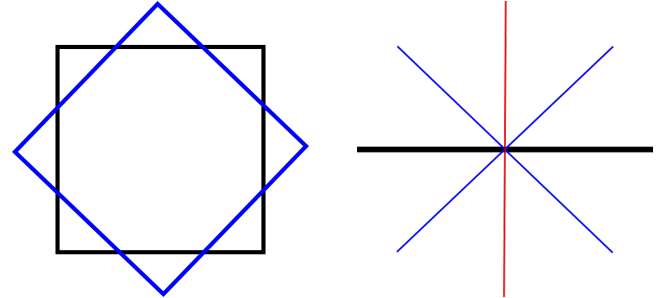
(a) Different orientations to close a square.

(b) Different orientations to zip to a line.

Figure 5: Different ways to close the end of a cylinder. As a convention, the black line indicates the base (bottom side) of the solid.

gluings. Another property is that all of the resulting polyhedra are combinatorially equivalent, in the sense that their 1-skeleton graphs are identical (K_4), except for two gluings into degenerate doubly covered rectangles.

In our results, as well as in past common unfolding results [6, 1, 8], the constructed polyhedra all have different gluing trees, and do not use continuous rolling belts. This is an indicator of the non-triviality of these solutions.

2.2 Comparison to Box Unfoldings

We claim that the box unfoldings in [6, 1, 8] are all countably infinite, up to scaling.

For instance, consider the construction in [8], which results in a common development of two boxes of size $a \times b \times 8a$ and $a \times 2a \times (2a + 3b)$. An important point to note here is that the construction requires tabs of a specific size. These tabs need to exactly divide both a and b into an integral number of pieces. Thus b/a has to be rational.

Because we are ignoring scale factors, we can set $a = 1$ without loss of generality. So, the number of common developments possible in this setting is just the number of possible values of b, which is a subset of the rationals. Therefore, we obtain a countable family of developments. (Of course, if we reintroduce scale factors, each member of this family will correspond to an uncountably infinite number of scaled copies, one for each positive real number a.)

3 Square Prism

A square prism is a cuboid where one set of opposite faces are squares. So, a square prism is a cuboid of size $a \times a \times b$. For the remainder of this paper, we will abbreviate this as an $a \times b$ prism.

Definition 3.1. The *aspect* ratio of an $a \times b$ prism is defined as b/a.

Starting with the two possible cylinders (Figure 4), we can close both ends to make corresponding squares (as in Figure 3b) to obtain two square prisms with different aspect ratios (Figure 6). The crease patterns are in Figure 2a.

- The prism resulting from closing the L-cylinder has aspect ratio $(W - L/8) \times (L/4) = \left(\frac{4}{L} - \frac{1}{2}\right) \times 1$.

- The prism resulting from closing the W-cylinder has aspect ratio $(L - W/8) \times (W/4) = \left(4L - \frac{1}{2}\right) \times 1$

We can compare the two prisms formed by plotting their aspect ratios with respect to the aspect ratio of the starting development; see Figure 7. This gives us the following theorem.

Theorem 2. *Given any aspect ratio $\alpha \in (0, 31.5) \setminus \{3.5\}$, we can construct an unfolding of a prism with aspect ratio α such that the unfolding also folds into a prism with a different aspect ratio. This results in an uncountably infinite family of common unfoldings.*

Proof. If $\alpha \in (0, 3.5)$, then we set $L = \frac{4}{\alpha + 0.5}$, and if $\alpha \in (3.5, 31.5)$, then we set $L = \frac{\alpha + 0.5}{4}$. This ensures that $1 < L < 8$. Since $L \neq 1$, we can ensure that the two prisms formed have distinct aspect ratios ($4L - 0.5$ and $4/L - 0.5$). Recall that we ignore scale factors by setting $W = 1$. □

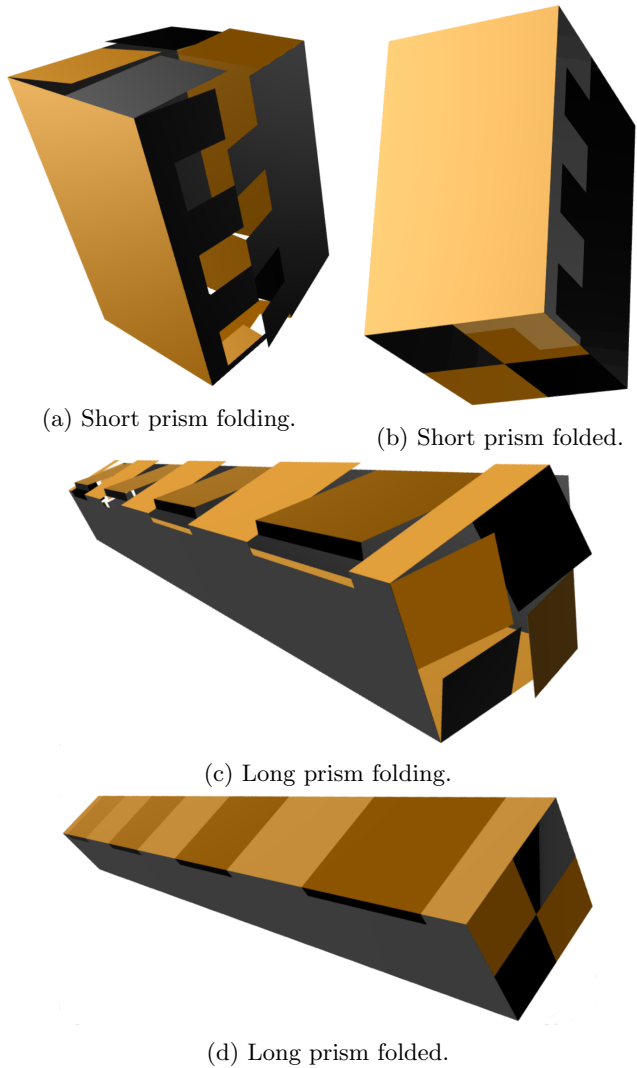(a) Short prism folding.

(b) Short prism folded.

(c) Long prism folding.

(d) Long prism folded.

Figure 6: Two different square prisms from a common development.
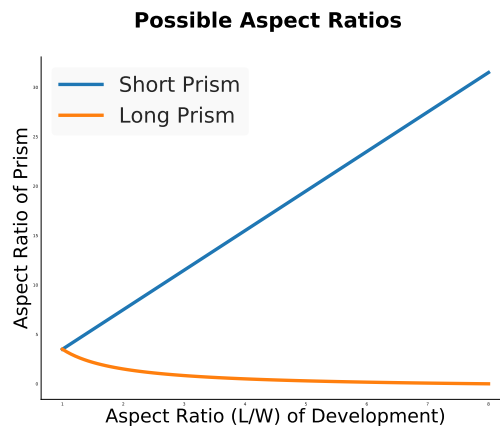
Possible Aspect Ratios

Figure 7

3.1 Anti-prisms

We saw in Figure 3c that we can close a cylinder end into a square that is rotated by 45°. This implies that we can close both end-caps into squares that are offset by a "half-turn". This construction results in a square anti-prism. The two square faces of the anti-prism will be oriented as the blue and black squares in Figure 5a.
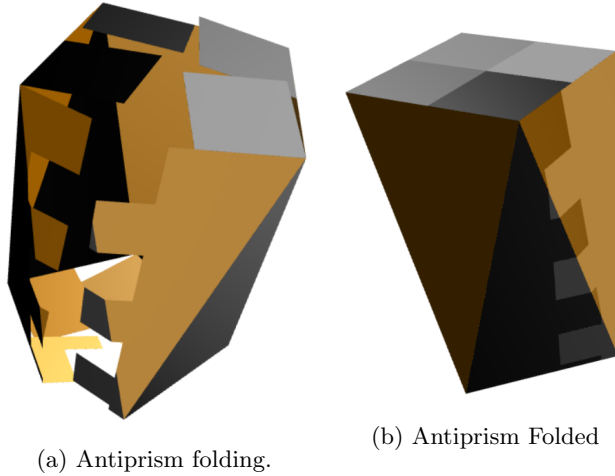

(a) Antiprism folding.

(b) Antiprism Folded

Figure 8: Folding the short anti-prism.

As before, we can obtain a short anti-prism by starting with the L-cylinder and a long one by starting with the W-cylinder. A partially folded anti-prism is shown in Figure 8a and the final folded form is in Figure 8b. Both crease patterns are shown in Figure 2c.

4 Isosceles Tetrahedra

Next, we will consider the solids that are formed by zipping the ends of a cylinder into a line (Figure 3a). Note that we can zip the line in one of four different orientations (Figure 5b). If we let the two ends zip according to the black and red lines in Figure 5b, we obtain a tetrahedron with isosceles faces.

We can construct two different sizes of tetrahedra by starting with either the L or the W cylinder. Both of the possible tetrahedra along with their partially folded states are shown in Figure 9. The crease patterns are in Figure 2d.

Definition 4.1. The *aspect ratio* of an isosceles tetrahedron is defined as the ratio of the height of the isosceles triangle to the length of its base.

The short tetrahedron has an aspect ratio of $L/2 \times W = L \times 2$ and the long tetrahedron has an aspect ratio of $W/2 \times L = 2 \times L$

Theorem 3. *For any aspect ratio $\alpha \in (0.25, 4) \setminus \{2\}$, there is a common unfolding of an α-tetrahedron and a distinct tetrahedron (having different aspect ratio).*

(a) Short tetrahedron folding.

(b) Short tetrahedron folded.

(c) Long tetrahedron folding.

(d) Long tetrahedron folded.
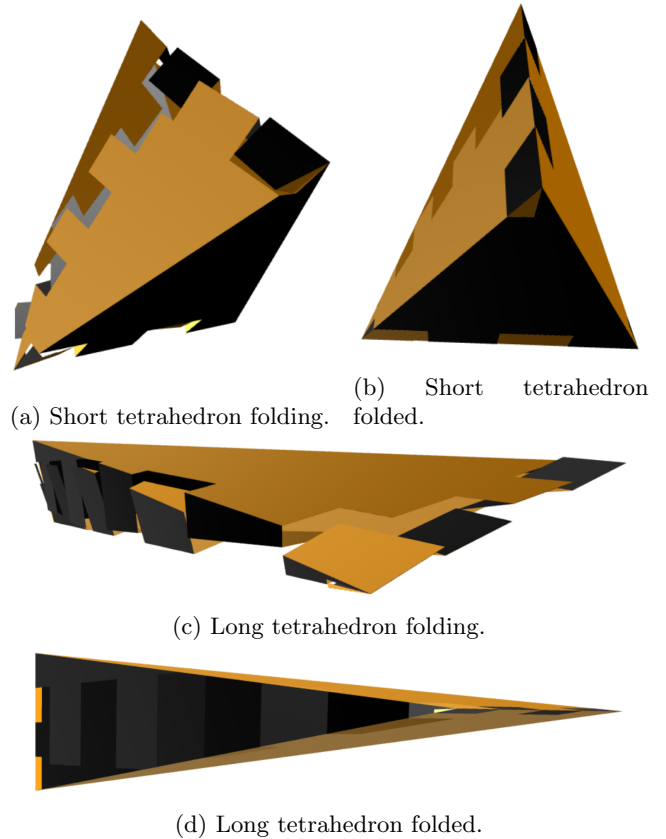
Figure 9: Folding tetrahedra

Proof. We set $L = 2/\alpha$ if $\alpha < 2$ and $L = 2\alpha$ if $\alpha > 2$. Since $L \neq 2$, this results in two different prisms ($L/2$ and $2/L$). $\square$

4.1 Rhombic Disphenoid

We can also obtain non-isosceles tetrahedra by zipping the two ends of a cylinder into non-orthogonal lines. So, we can zip the two ends according to the black and blue lines in Figure 5b.
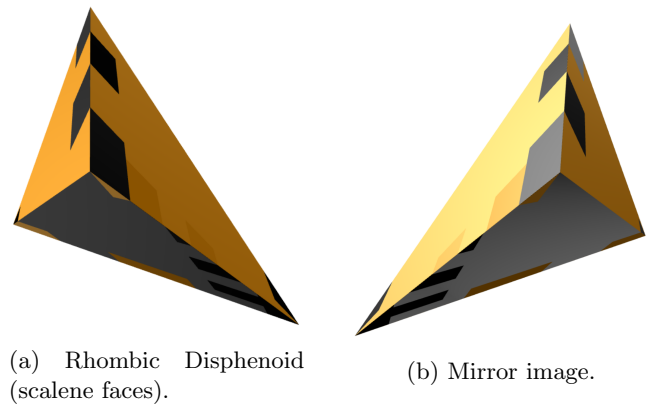

(a) Rhombic Disphenoid (scalene faces).

(b) Mirror image.

Figure 10

This construction results in a tetrahedron with congruent scalene triangle faces. This is also called a *rhombic disphenoid*. This is the only polyhedron in this paper that is chiral, and we can form the mirror image by turning the unfolding "inside-out". Both versions of the disphenoid are shown in Figure 10. The crease patterns for both the long and the short disphenoid are in Figure 2e.

5 Obtuse Wedges

In addition to zipping both ends of the cylinder in an equivalent way, we can also zip one end to a line and the other end to a square. This gluing results in a polyhedron with a square base, two triangular side faces, and two trapezoidal side faces (Figure 11). This solid is an obtuse wedge. Both of the crease patterns are shown in Figure 2b.
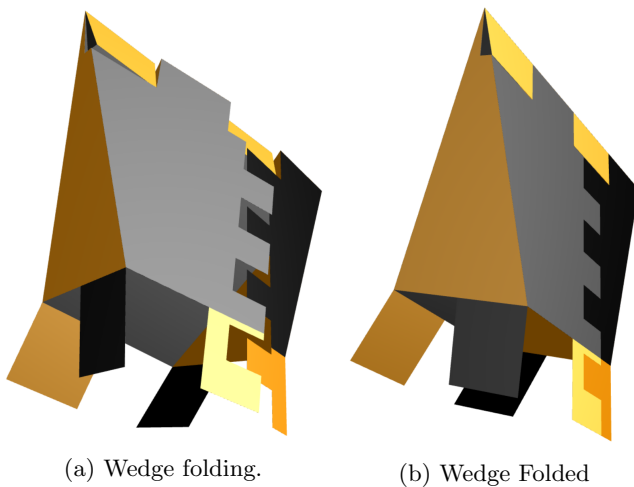

(a) Wedge folding.
(b) Wedge Folded

Figure 11: Zipping two ends differently results in a wedge (half a tetrahedron). The four bottom tabs have to be folded up to complete the square base.

The wedge can also be thought of as a "half tetrahedron": when we extend four side edges, we eventually obtain a tetrahedron (Figure 12). The aspect ratio (Definition 4.1) of this tetrahedron extension is $(W - L/16) \times (L/4) = (16 - L) \times 4L$ for the short wedge, and $(L - W/16) \times (W/4) = (16L - 1) \times 4$ for the long wedge (using $W = 1$).
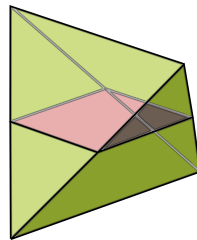

Figure 12: Two wedges forming a tetrahedron.

6 Conclusion

In this paper, we constructed an uncountable family of common developments. Unlike the majority of previous results, these developments fold to more than three convex polyhedra. It may be possible to extend the basic ideas from the tab construction to other types of polygons and obtain more interesting unfolding families. As a bonus, our developments tile the plane, which has practical implications.

Acknowledgements

References

[1] Z. Abel, E. Demaine, M. Demaine, H. Matsui, G. Rote, and R. Uehara. Common developments of several different orthogonal boxes. In *The 23rd Canadian Conference on Computational Geometry (CCCG'11)*, 2011.

[2] G. Aloupis, P. K. Bose, S. Collette, E. D. Demaine, M. L. Demaine, K. Douïeb, V. Dujmović, J. Iacono, S. Langerman, and P. Morin. Common unfoldings of polyominoes and polycubes. In *Computational Geometry, Graphs and Applications*, pages 44–54. Springer, 2011.

[3] Y. Araki, T. Horiyama, and R. Uehara. Common unfolding of regular tetrahedron and Johnson-Zalgaller solid. In *Journal of Graph Algorithms and Applications, Vol.20, No.1*, pages 101–114, 2016.

[4] E. D. Demaine and J. O'Rourke. *Geometric Folding Algorithms*. Cambridge University Press, 2007.

[5] A. Lubiw and J. O'Rourke. When can a polygon fold to a polytope. In *Technical Report Technical Report 048, Department of Computer Science, Smith College*, 1996.

[6] J. Mitani and R. Uehara. Polygons folding to plural incongruent orthogonal boxes. In *Proc. CCCG*, pages 31–34, 2008.

[7] T. Shirakawa, T. Horiyama, and R. Uehara. On common unfolding of a regular tetrahedron and a cube. pages 47–50, 2011.

[8] T. Shirakawa and R. Uehara. Common developments of three incongruent orthogonal boxes. In *International Journal of Computational Geometry and Applications, Vol. 23, No. 1*, pages 65–71, 2013.